

Multiphoton polarization imaging of the stratum corneum and the dermis in ex-vivo human skin

Yen Sun, Jiunn-Wen Su, Wen Lo

Department of Physics, National Taiwan University, Taipei 106, Taiwan

Sun-Jan Lin¹, Shiou-Hwa Jee^{1,2}

¹*Department of Dermatology, National Taiwan University Hospital, Taipei 106, Taiwan*

²*Department of Dermatology, National Taiwan University College of Medicine, Taipei 106, Taiwan*

Chen-Yuan Dong

Department of Physics, National Taiwan University, Taipei 106, Taiwan

cydong@phys.ntu.edu.tw

Abstract: Abstract: In this work, we demonstrate the application of multiphoton polarization imaging in resolving the structures in surface stratum corneum and dermal layers of ex-vivo human skin. By varying the excitation and emission polarizations, we characterized the structural features in both Laurdan labeled stratum corneum and dermal fibers. The results presented here have important consequences in bioimaging applications of the skin. Both the mechanics of transdermal drug delivery across the skin and physiological significance of the structural changes of the dermis can be monitored. Our results show that the transition dipoles of Laurdan molecules are preferentially oriented normal to the membrane surface. Furthermore, polarization imaging shows that fibrous structures in the dermis generate emission aligned strongly along the excitation polarization. This work shows that multiphoton polarization imaging can be a powerful method in identifying structural orientations in the skin and other biological structures.

©2003 Optical Society of America

OCIS codes: (180.2520) Fluorescence microscopy; (170.1870) Dermatology

References and links

1. W. Denk, J. H. Strickler, and W. W. Webb, "Two-photon laser scanning fluorescence microscopy," *Science* **248**, 73-76 (1990).
2. P. T. C. So, C. Y. Dong, B. R. Masters, and K. M. Berland, "Two-photon excitation fluorescence microscopy," *Annual Review of Biomedical Engineering* **2**, 399-429 (2000).
3. J. R. Lakowicz, *Principles of fluorescence spectroscopy* (Kluwer Academic/Plenum Publishers, 1999) Chaps. 10,11,12.
4. L. A. Bagatolli and E. Gratton, "Two photon fluorescence microscopy of coexisting lipid domains in giant unilamellar vesicles of binary phospholipids mixtures," *Biophysical J.* **78**, 290-305 (2000).
5. P. Stoller, K. M. Reiser, P. M. Celliers, and A. M. Rubenchik, "Polarization-modulated second harmonic generation in collagen," *Biophysical J.* **82**, 3330-3342 (2002).
6. P. Stoller, B. M. Kim, A. M. Rubenchik, K. M. Reiser, and L. B. Da Silva, "Polarization-dependent optical second-harmonic imaging of a rat-tail tendon," *J. Biomed. Opt.* **7**, 205-214 (2002).
7. A. Y. Yeh, N. Nassif, A. Zoumi, and B. J. Tromberg, "Selective corneal imaging using combined second-harmonic generation and two-photon excited fluorescence," *Opt. Lett.* **27**, 2082-2084.
8. B. Yu, C. Y. Dong, P. T. C. So, D. Blankschtein, and R. Langer, "In vitro visualization and quantification of oleic acid induced changes in transdermal transport using two-photon fluorescence microscopy," *J. Investigative Dermatology* **117**, 16-25 (2001).

9. B. Yu, K. H. Kim, P. T. C. So, D. Blankschtein, and R. Langer, "Topographic heterogeneity in transdermal transport revealed by high-speed two-photon microscopy: determination of representative skin sample sizes," *J. Investigative Dermatology* **118**, 1085-1088 (2002).
10. B. Yu, K. H. Kim, P. T. C. So, D. Blankschtein, and R. Langer, "Visualization of oleic-acid induced transdermal diffusion pathways using two-photon fluorescence microscopy," *J. Investigative Dermatology* **120**, 448-455 (2003).
11. T. Parasassi, G. De Stasio, G. Ravagnan, R. M. Rusch, and E. Gratton, "Quantitation of lipid phases in phospholipids vesicles by the generalized polarization of Laurdan fluorescence," *Biophys. J.* **60**, 179-189 (1991).

1. Introduction

1.1 Advantages of multiphoton excitation microscopy

Since its introduction in 1990, two-photon fluorescence microscopy has evolved into one of the major imaging techniques in optical microscopy [1]. In this technique, fluorescent molecules excitable by the one-photon excitation process are induced to absorb two less energetic photons in reaching the excited state. As a result, UV or visible absorbing fluorophores may be induced to absorb two near-infrared photons in reaching the excited state. The multiphoton approach has proven to be advantageous in many ways. First, the non-linear process responsible for multiphoton excitation results in limiting sample excitation to the focal volume. As a result, confocal-like imaging quality can be achieved without using detection apertures. Furthermore, point-like excitation also limits sample damage to the focal volume resulting in improved specimen longevity. The second major advantage of multiphoton biological microscopy is its ability to image deep within three-dimensional specimens. Unlike the UV or visible photons used in one-photon excitation, the near-infrared photons used in multiphoton microscopy are absorbed and scattered less by tissue components. Therefore, the multiphoton excitation source can be focused more deeply into biological specimens. It is this feature that allows in-depth examination of biological specimens at high resolution [2].

1.2 Combining polarization imaging with multiphoton microscopy

Although multiphoton excitation microscopy has been successfully applied to investigate a wide of biological specimens, its combination with polarization methods can lead to additional insights. In conventional polarization methodology, the orientation properties of a specimen can be investigated by exciting the specimen with polarized light. The fluorescence emission is then observed at polarization angles parallel (\parallel) and perpendicular (\perp) to the excitation polarization axis. By defining the polarization p and r respectively as

$$p = \frac{I_{\parallel} - I_{\perp}}{I_{\parallel} + I_{\perp}} \text{ and } r = \frac{I_{\parallel} - I_{\perp}}{I_{\parallel} + 2I_{\perp}}, \quad (1)$$

the sample excitation and emission dipole orientations can be determined. Fluorescence polarization spectroscopy based on this approach has been successful in revealing the dynamics of chromophores in solution [3].

By combining multiphoton excitation and polarization techniques in biological microscopy, one can expect to obtain in-depth, structural information obscured by intensity imaging alone. However, the traditional approach based on polarization or anisotropy techniques described by Eqn. 1 requires modification. In conventional spectroscopic approach, the sample fluorophores is distributed in random orientations. The measured polarization or anisotropy values represent an average characteristic of the specimen. Since a continuum of fluorophore orientations was present, a single polarization direction is adequate for sample excitation. In fact, since the fluorescence emission along the two perpendicular axes is equivalent, the denominator $I_{\parallel} + 2I_{\perp}$ in the definition of anisotropy r is physically significant in that it represents the total fluorescence emission. However, in polarization microscopy, it may not be adequate to have a fixed excitation polarization axis. The structural

heterogeneity in biological specimens dictates that, with inappropriate excitation polarization, the alignment of the fluorescent molecules within the samples may result in poor excitation. For example, it has been demonstrated that the probe Laurdan orients preferentially in artificial membranes with its transition dipole perpendicular to the membrane surface [4]. Another example is the second harmonic signal generated from collagen which has been shown to have a major component along the fiber axis. In these cases, it is evident that the excitation polarization axis needs to be chosen in matching the sample features being investigated [5,6,7].

1.3 Multiphoton polarization imaging of the skin

In this work, we investigate the polarization properties of ex-vivo human skin. In particular, we focused on two structures of the skin: the surface stratum corneum and the dermal fibers. There are two reasons these two features were chosen for our study. First, it is likely that both structures are highly polarized. The stratum corneum is known to contain membrane-like structures. On the other hand, collagen, a major component of the dermis, is known to be a highly polarized structure [5,6,7]. Secondly, any technique leading to a better characterization of the stratum corneum and dermis can have important biomedical consequences. To be specific, the microscopic barrier properties of the stratum corneum in transdermal drug delivery has been extensively investigated using multiphoton fluorescence microscopy [8,9,10]. Possible structural changes revealed by polarization microscopy can have important consequences in developing more efficient drug delivery methodologies. On the other hand, the process of skin aging has been correlated to the changes of dermal fibrous structures. In this area, if polarization microscopy can lead to dermal imaging with superior contrasts, it can assist in the characterization of the aging process in-vivo and lead to methodologies countering the effects of aging.

2. Materials and methods

2.1 Components of a multiphoton polarization microscope

The design of our multiphoton polarization microscope is shown in Fig. 1. A 10 W diode (Millenia X, Spectra Physics, Mountain View, CA) pumped titanium sapphire laser (Tsunami, Spectra Physics) was used as the excitation source. The laser is guided to an upright microscope (E800, Nikon, Japan) by optical components intended to guide and control the power and polarization of the excitation beam. The laser beam passes through a half-wave plate prior to reaching a polarizer (CVI Laser, Albuquerque, NM). By rotating the half-wave plate, the excitation power may be changed without altering the excitation polarization. Next, the angular deviation of the polarized excitation beam is controlled by an x-y scanner system (Model 6220, Cambridge Technology, Cambridge, MA). The scanned beam is expanded by a pair of lenses and then reflected into the back aperture of the objective (S-Fluor 40x, NA 1.4, Nikon) by a short-pass dichroic mirror (720DCSPXR, Chroma Technology, Brattleboro, VT). The beam expansion ensures overfilling of the objective's back aperture and results in a tightly focused excitation spot. The emission generated is collected in the epi-illuminated fashion and is passed through the dichroic mirror and an additional short-pass filter (E680SP, Chroma Technology) before being guided to a polarizer situated in front of a single-photon counting PMT (R7400P, Hamamatsu, Japan). With the short-pass dichroic mirror and filter selected, we perform broad-band detection of sample emission. To acquire the polarization images, both the polarizations of the excitation beam and the emission polarization axis were altered. Both polarization directions (vertical and horizontal to the image orientation) can be chosen by altering the excitation polarizer situated outside of the microscope system. In this process, the half-wave plate is also rotated to ensure equal power in the excitation beam in switching between the two excitation polarizations. In addition, the emission polarization is also altered between the axes parallel and perpendicular to the excitation directions. To calibrate the orientation of the emission polarizer relative to that of the excitation polarization, a mirror was placed at the objective's focal plane and the short pass E680SP filter was

removed to allow partial passage of the reflected excitation beam in reaching the PMT. The parallel (relative to the excitation beam) orientation of the emission polarizer is then set by rotating the emission polarizer until a maximum signal is registered at the PMT. The perpendicular (relative to the excitation beam) beam can be determined by rotating the emission polarizer until a minimum PMT signal is recorded.

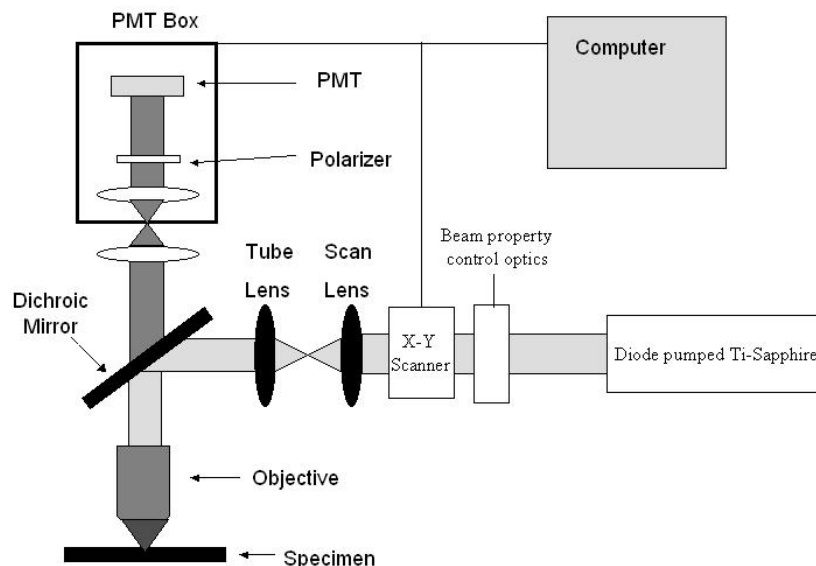


Fig. 1 A multiphoton polarization microscope

2.2 Ex-vivo skin preparation

Two types of ex-vivo skin samples were prepared. The first sample is an excised skin specimen labeled with the membrane probe 6-dodecanoyl-2-dimethylaminonaphthalene (Laurdan, D-250, Molecular Probes, Eugene, OR). To prepare the solution for skin treatment, a stock solution of 1.9 mM Laurdan (12 mg in 17.7 ml of DMSO) was made. The skin treatment solution was prepared by diluting 10 μ l of the Laurdan/DMSO stock in 1 ml of PBS buffer (pH 7.4). The excised human skin was then soaked in the treatment solution for 11 hours at room temperature. The Laurdan-treated skin was wrapped in aluminum foil for shielding from room light. At the end of the treatment period, the skin sample is removed and rinsed with PBS buffer and mounted on a microscope slide for viewing. The absorption (one-photon) and emission properties of Laurdan have been extensively studied. In general, Laurdan absorbs in the 300-400 nm range and emits in the 400-500 nm range.[11] To prepare the dermal fiber skin specimen, a piece of excised skin is mounted on a microscope slide for viewing. In both specimens, the skin was mounted using a piece of silicone sheet (Press-to-Seal, P-24745, Molecular Probes). A hole was cut near the center of the silicone piece where the skin is positioned. To maintain the moisture of the skin, a wet piece of paper tissue was sandwiched between the skin and glass slide. Both samples were sealed with No. 1.5 thick cover glasses.

3. Results and discussions

With the Laurdan-treated specimen, our focus was on the polarization images of Laurdan molecules present at the membrane of the surface stratum corneum. We obtained polarization-resolved images of the same area within the Laurdan-treated stratum corneum by varying the orientations of both the excitation and emission polarizers. The images are shown in Fig. 2.

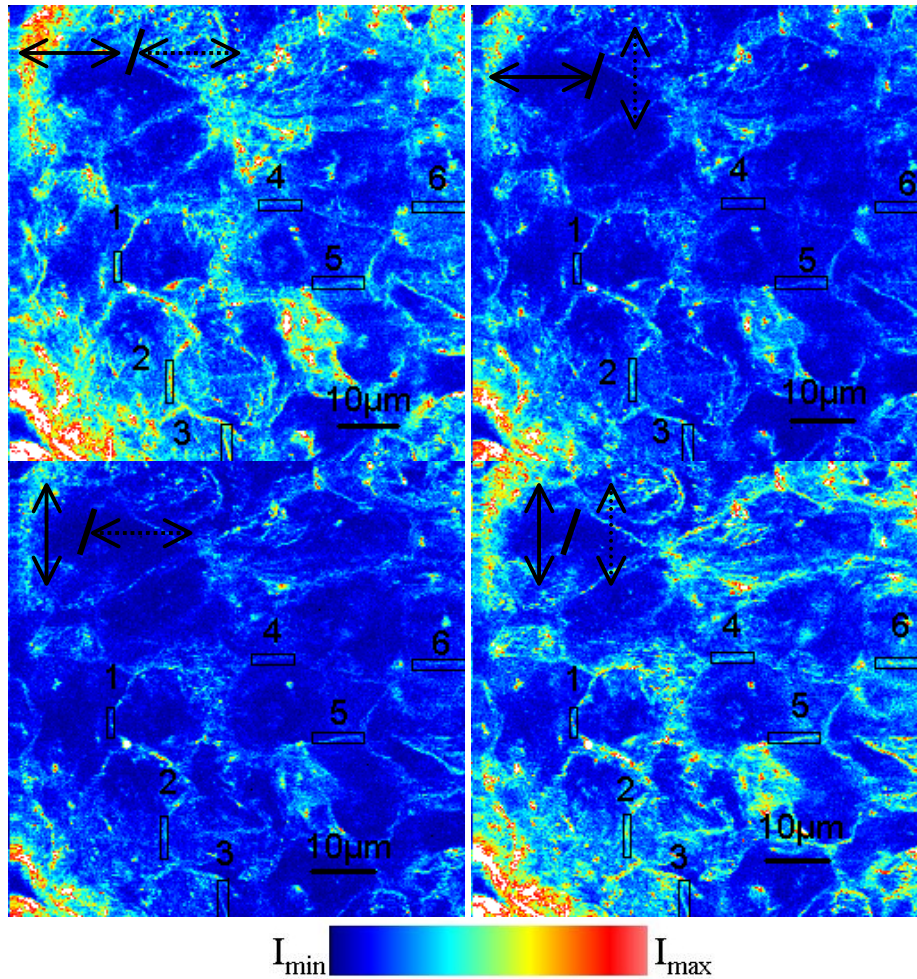


Fig. 2. Polarization-resolved images of laurdan treated stratum corneum ($I_{\max}=150$, $I_{\min}=0$)

In images presented in Fig. 2, the orientation of the excitation polarization is indicated as solid-line arrows and that of the emission channel is indicated as dashed arrows. In the top two figures, the excitation polarization is along the horizontal axis and the emission polarization is varied between the horizontal axis (top left) and the vertical axis (top right). In the bottom two images, the excitation polarization is along the vertical axis while that of the emission polarizer is along the horizontal (bottom left) and vertical (bottom right) directions. It has been shown that the transition dipole of Laurdan is perpendicular to the membrane [4]. Therefore, to selectively excite membranes along the vertical axis, a horizontal excitation polarization is needed. On the other hand, a vertical excitation polarization is needed to excite the Laurdan molecules located in the horizontally oriented membranes of the stratum corneum. In our study, by varying the emission polarizer orientations, we can obtain the polarization values of Laurdan in the stratum corneum membrane. To do this, we selected six regions of the membrane part of the stratum corneum images. Three of them (1, 2, and 3) have vertical orientations while the remaining three (4, 5, and 6) are positioned horizontally. To obtain the average polarization values of the vertically and horizontally oriented membranes, we averaged the polarization values of the three regions of each membrane orientation calculated according to Eqn. (1). And the results are shown in Table 1. As Table 1 shows, the polarization value for the membrane region oriented perpendicular to the excitation polarization has larger P. To be specific, the respective average P values of the vertical and

horizontal membrane orientations are 0.27 ± 0.06 and 0.21 ± 0.06 for horizontal excitation. Polarization was also calculated for vertical excitation and its value is 0.35 ± 0.08 for horizontal membrane orientation and 0.30 ± 0.07 for vertical membrane polarization. These observations support the fact that the transition dipole moments of Laurdan are preferentially oriented perpendicular to the membrane surface.

The second sample we studied was unlabeled skin. In this specimen, we focused on imaging the fibrous structures in the dermis. The excitation and emission polarizations were altered in the same ways as for Laurdan labeled stratum corneum and the results are shown in Fig. 3. Six regions with two orthogonal fiber orientations were chosen for polarization calculations. Three areas in which the fibers were oriented vertically (1, 2, and 3) and another three areas (4, 5, and 6) with the fibers oriented horizontally were selected and the corresponding polarization values were calculated. The fibrous structures in our images demonstrate strong dependence of the emission along the direction of the excitation beam. In comparing the emission intensity of the fibrous regions, Fig. 3 shows that the emission is more intense when the emission polarizer is oriented parallel to the excitation direction. On the other hand, an examination of the calculated polarization values (shown in Table 1) shows that there is little correlation between fiber orientation and the polarization values. Our observation supports the conclusion that the observed emission from the fibers has strong dependence on the excitation polarization. However, the resolution of our images does not permit us to fully characterize the orientation of the dipoles within the fibers.

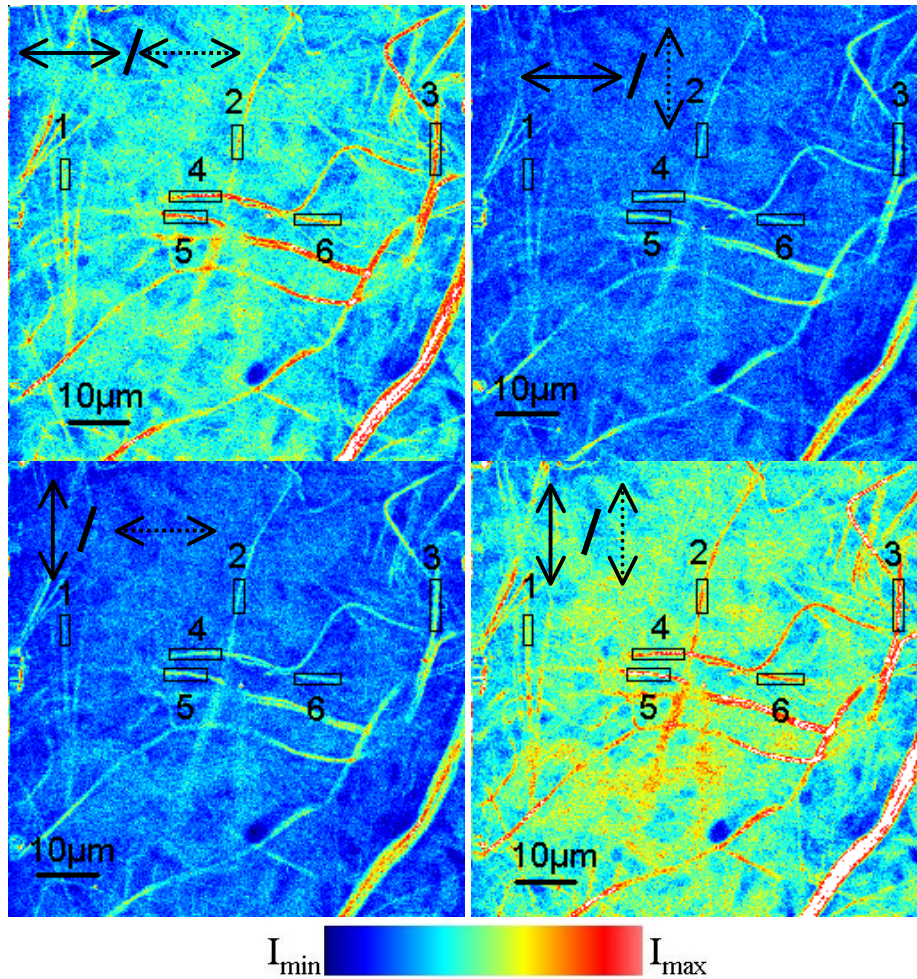


Fig. 3. Multiphoton polarization imaging of skin dermal fiber layers ($I_{\max}=100$, $I_{\min}=0$)

Table 1. Polarization values of Laurdan labeled stratum corneum and dermal fibers

Dermal Fibers					Stratum Corneum (Laurdan)				
excitation polarization	fiber orientation	area	P	P average	excitation polarization	membrane orientation	area	P	P average
\longleftrightarrow	\updownarrow	1	0.29 ± 0.10	0.27 ± 0.08	\longleftrightarrow	\updownarrow	1	0.31 ± 0.12	0.27 ± 0.06
		2	0.24 ± 0.16				2	0.25 ± 0.13	
		3	0.28 ± 0.12				3	0.27 ± 0.08	
	\longleftrightarrow	4	0.27 ± 0.12	0.27 ± 0.07		\longleftrightarrow	4	0.21 ± 0.12	0.21 ± 0.06
		5	0.27 ± 0.13				5	0.20 ± 0.10	
		6	0.28 ± 0.13				6	0.22 ± 0.11	
\updownarrow	\updownarrow	1	0.37 ± 0.11	0.35 ± 0.06	\updownarrow	\updownarrow	1	0.33 ± 0.16	0.30 ± 0.07
		2	0.35 ± 0.10				2	0.29 ± 0.10	
		3	0.34 ± 0.10				3	0.30 ± 0.11	
	\longleftrightarrow	4	0.34 ± 0.10	0.33 ± 0.06		\longleftrightarrow	4	0.36 ± 0.10	0.35 ± 0.08
		5	0.32 ± 0.11				5	0.35 ± 0.17	
		6	0.33 ± 0.11				6	0.33 ± 0.11	

4. Conclusion

In this work, we demonstrated multiphoton polarization imaging of Laurdan labeled stratum corneum and emission from dermal fibers. Our results show that Laurdan molecules can be used on skin surface imaging and can also be used to identify membrane orientation of the skin. Combined with the interested delivery enhancement methodologies, multiphoton techniques can be used to elucidate the mechanisms of transdermal delivery. We also showed that emission from dermal fibers within human skin have strong correlation to the excitation polarization direction. However, the fiber emission does not have high correlation to its orientation, indicating that the resolution of our images does not permit a determination of the relation between the transition dipoles to the fiber orientation. Nonetheless, the polarization technique demonstrated in this work can be used to diagnose fiber emission in the dermal layers and can have potential application in skin physiological studies.

Acknowledgments

We wish to acknowledge the support of NSC 92-2112-M-002-018 (National Science Council, Taiwan) for this project.